Diorganotin(IV) derivatives of salicylaldehydethiosemicarbazone. The crystal structure of dimethyl- and diphenyl-(salicylaldehydethiosemicarbazonato)tin(IV)

J.S. Casas*, A. Sánchez, J. Sordo and A. Vázquez-López
Departamento de Química Inorgánica, Universidade de Santiago de Compostela, 15706 Santiago de Compostela (Spain)

E.E. Castellano and J. Zukerman-Schpector
Instituto de Fisica e Quimica de Sao Carlos, USP, CEP13560 Sao Carlos (Brazil)

M.C. Rodríguez-Argüelles
Departamento de Química Pura e Aplicada, Universidade de Vigo, 36200 Vigo (Spain)

U. Russo
Dipartamento di Chimica Inorganica, Metallorganica ed Analitica, Università di Padova, 35131 Padua (Italy)

(Received July 9, 1993; revised September 28, 1993)

Abstract

The title compounds have been prepared by reacting the corresponding diorganotin(IV) oxide with salicylaldehyde thiosemicarbazone (H_2L). [$SnMe_2(L)$] crystallizes in the monoclinic space group $P2_1/n$ with $a = 9\,480(3)$, $b = 13.532(7)$, $c = 10.541(3)$ Å, $\beta = 100.33(2)°$ and $Z = 4$ ($R = 0.0230$, $R' = 0.0258$). [$SnPh_2(L)$] crystallizes in the space group $P2_1/a$ with $a = 13.483(8)$, $b = 10.078(1)$, $c = 15.622(4)$ Å, $\beta = 113.66(4)°$ and $Z = 4$ ($R = 0\,030$, $R' = 0.031$). Both complexes consist of molecules in which the bisdeprotonated ligand is O,N,S-bonded and the tin atom exhibits distorted pentacoordination, with small differences between the methyl and phenyl derivatives in bond distances, bond angles and intermolecular hydrogen bonds. The spectral properties of the complexes (IR, Mossbauer and ^1H, ^{13}C and ^{119}Sn NMR spectra) are discussed in the light of this structural information.

Key words: Crystal structures; Tin complexes; Organotin complexes, Thiosemicarbazone complexes

Introduction

Thiosemicarbazones possess a range of interesting pharmacological properties that are in some cases enhanced in their metallic derivatives. This fact has prompted a considerable increase in the study of the coordination behaviour of these ligands in recent years [1]. Bearing in mind that diorganotin(IV) compounds too have significant biological applications [2], we decided to explore the chemistry and pharmacological activity of diorganotin thiosemicarbazonates [$SnR_2(L)$], where H_2L is salicylaldehyde thiosemicarbazone and R = Me or Ph. Some previous work has been done in this field [3, 4] including the synthesis and spectroscopic (mainly IR) study of [$SnPh_2(L)$] [4b]. We report here the crystal structure of [$SnMe_2(L)$] and [$SnPh_2(L)$] and, in the light of this information, we discuss the spectral behaviour of these complexes in the solid state and in solution, using IR, Mossbauer and ^1H, ^{13}C and ^{119}Sn NMR spectroscopy to establish structural–spectral correlations. As far as we know, this is the first X-ray diffraction study of a salicylaldehyde thiosemicarbazonate of a main group element.

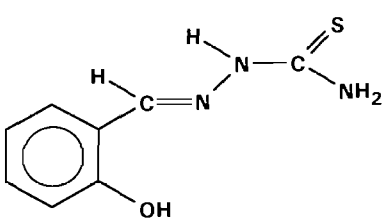

*Author to whom correspondence should be addressed.

SSDI 0020-1693(93)03724-O

Experimental

Thiosemicarbazide (Merck), salicylaldehyde (Merck), dimethyltin dichloride (Alfa) and diphenyltin dichloride (Aldrich) were used as supplied. The ligand H_2L and the diorganotin(IV) oxides were obtained by the procedure described in ref. 5a and 5b, respectively. Elemental analyses were performed with a Carlo Erba 1108 analyser. Melting points were determined with a Buchi apparatus. IR spectra were recorded in KBr pellets on a Perkin-Elmer 1330 spectrometer The mass spectra were obtained using a Kratos MS50TC spectrometer connected to a DS90 data system and operating in electron impact (EI) mode (direct insertion probe, 70 eV, 250 °C); all the fragments were identified using DS-90 software. ^1H, ^{13}C and ^{119}Sn NMR spectra were recorded at room temperature on a Bruker WM250 instrument and were referred to the solvent signal (^1H, 7.27 and 2.48; ^{13}C, 77.00 and 39.51 ppm for $CDCl_3$ and DMSO-d_6, respectively) and to neat $SnMe_4$ as external reference. The Mössbauer spectra were recorded at 80 K in a constant acceleration apparatus and δ was referred to r.t. SnO_2.

Synthesis of [$SnMe_2$(L)]

Dimethyltin(IV) oxide (0.50 g, 3 mmol) and H_2L (0.49 g, 3 mmol) were suspended in 100 ml of benzene (**caution**) in a 250 ml, two-neck, round-bottomed flask fitted with a Dean-Stark moisture trap and condenser. The reaction mixture was refluxed for 5 days and the solid residue removed by filtration. After cooling and slow concentration of the clear solution, a crystalline solid formed that was isolated and vacuum dried. M.p. 150 °C. *Anal.* Found: C, 35.8; H, 3.9; N, 12.4 Calc. for $C_{10}H_{13}N_3OSSn$: C, 35.1; H, 3.8; N, 12.3%.

Synthesis of [$SnPh_2$(L)]

The same procedure was used for preparing the diphenyltin analogue. H_2L (0.28 g, 1.4 mmol) and diphenyltin(IV) oxide (0.40 g, 1.4 mmol) were suspended in 100 ml of benzene (**caution**) and refluxed for 5 days in a 250 ml, two-neck, round-bottomed flask fitted with a Dean-Stark trap. After removal of the solid residue by filtration, the solution was slowly concentrated until a crystalline solid formed which was filtered off and dried under vacuum. M.p. 130 °C. *Anal.* Found: C, 50.9; H, 3.8; N, 8.3. Calc. for $C_{20}H_{17}N_3OSSn$: C, 51.5; H, 3.7; N, 9.0%. This compound has the same analytical composition as the product isolated before [4b] by different synthetic routes, but the m.p. observed in our work differs from the decomposition temperature quoted by Nath *et al.* [4b], and the ^1H NMR spectrum of our complex after melting and resolidification shows no change indicating decomposition.

Crystal structure determinations

All X-ray crystallography was carried out using an Enraf-Nonius CAD-4 diffractometer with graphite-monochromated Mo Kα radiation ($\lambda = 0.71073$ Å). The intensity of three standard reflections was essentially constant throughout the experiments. Crystal data and experimental conditions are listed in Table 1. Final atomic coordinates are listed in Tables 2 and 3.

Structures were solved using the standard heavy atom Patterson method and difference Fourier techniques In final cycles of full-matrix least-squares refinement all non-H atoms were treated anisotropically H atoms were included, as fixed contributors, at positions found in difference synthesis (slightly modified, when necessary, on stereochemical grounds), all with a common isotropic temperature factor that refined to $U = 0.081(3)$ Å^3 ([$SnMe_2$(L)]) or 0.094(5) Å^3 ([$SnPh_2$(L)]). Data were corrected for Lp and absorption [6]. The programs and the computer used, sources of scattering factors and corrections for anomalous dispersion for non-H atoms are given in ref. 7 Scattering factors for H atoms were taken from ref. 8.

Results and discussion

Crystal structures of the complexes

In both complexes the ligand is tridentate via its sulfur, N(3) and oxygen atoms (Figs. 1 and 2), giving a coordination polyhedron around the tin atom that can be described as a distorted trigonal bipyramid with the ligand occupying the two axial positions and one equatorial position. The value of the C–Sn–C angle makes the description involving *trans* axial phenyl groups which has been proposed on spectroscopic grounds [4b], untenable.

As in other complexes of tridentate thiosemicarbazones [9], the main distortion from regular bipyramidal geometry comes from the stereochemical limitations of the ligand, which reduce the S–Sn–O angle from the ideal value of 180° to the values of 158.10(5) and 161.1(1)° observed in [$SnMe_2$(L)] and [$SnPh_2$(L)], respectively. The low degree of planarity of the ligand in the dimethyltin complex (see below) also contributes to the distortion. The Sn–O and Sn–N distances (Tables 4 and 5) are close to the sums of the non-polar covalent radii (2.13 and 2.15 Å, respectively [10]) indicating strong bonds. The Sn–S distance, though longer than the sum of the non-polar covalent radii (2.42 Å) [10] and than the Sn–S distance in the solely S-bound complex formed by triphenyltin(IV) and a rather similar thiosemicarbazone [11], is considerably shorter than the sum of the van der Waals radii (4.0 Å) [12], suggesting a fairly strong bond. The Sn–C distances are unremarkable [13]. A similar coordination kernel for the

TABLE 1 Crystal data, details of intensity measurements and structure refinement for $[SnR_2(L)]$ complexes

	$[SnMe_2(L)]$	$[SnPh_2(L)]$
Formula	$C_{10}H_{13}N_3OSSn$	$C_{20}H_{17}N_3OSSn$
M	341 99	466.13
Space group	$P2_1/n$	$P2_1/a$
a (Å)	9 480(3)	13.483(8)
b (Å)	13.532(7)	10.078(1)
c (Å)	10.541(3)	15 622(4)
β (°)	100.33(2)	113.66(4)
V (Å)^3	1330(2)	1945(2)
Z	4	4
D_{calc} (g cm^{-3})	1 707	1.592
Sample dimensions (mm)	0.50×0.45×0.20	0.26×0.17×0 10
λ(Mo Kα) (Å)	0.71073	0.71073
T (K)	293	293
Linear absorption coefficient, μ (cm^{-1})	20.62	14.33
Absorption correction max., min	1.19, 0.82	1 127, 0.841
Scan technique	$\omega/2\theta$	$\omega/2\theta$
h Range for data collection (°)	0–30	0–25
$F(000)$	672	928
No. reflections measured	4036	3090
No. of unique reflections	3665	3060
R_{int}	0 0212	0.016
No reflections above $3\sigma(I)$	3142	2292
Function minimized	$\Sigma w(\|F_o\|-\|F_c\|)^2$	$\Sigma w(\|F_o\|-\|F_c\|)^2$
Weighting scheme	$[r^2(F_o)+0\,0001\|F_o\|^2]^{-1}$	$[r^2(F_o)+0.0001\|F_o\|^2]^{-1}$
$R=\Sigma\|\|F_o\|-\|F_c\|\|/\Sigma\|F_o\|$	0 0230	0.030
$R'=[\Sigma w(\|F_o\|-\|F_c\|)^2/\Sigma w\|F_o\|^2]^{1/2}$	0.0258	0.031
$S=[\Sigma w(\|F_o\|-\|F_c\|)^2/(M-N)]^{1/2}$	1.72	1.52
h_{min}, h_{max}, k_{min}, k_{max}, l_{min}, l_{max}	−13.13, 0 18; 0.14	−16 14, 0.11, 0 18
Residual $\Delta\rho$ max, min. (e Å^{-3})	0 46, −0.42	0.48, −0.41

TABLE 2 Positional parameters for $[SnMe_2(L)]$ with e.s.d.s in parentheses

Atom	x/a	y/b	z/c	B_{iso}
Sn	0 2446(1)	0.0967(1)	0 0635(1)	3.184(5)
S	0 2367(1)	−0.0666(1)	0.1813(1)	5 50(3)
O	0 3074(2)	0 2428(1)	0.0307(2)	3 75(5)
C(1)	0.3558(3)	−0 0317(2)	0 3173(2)	3 35(7)
C(2)	0.5378(2)	0.1655(2)	0.2242(2)	3 42(7)
N(1)	0 3641(3)	−0.0904(2)	0 4204(2)	4 39(7)
N(2)	0 4395(2)	0 0462(2)	0 3296(2)	3 39(6)
N(3)	0.4282(2)	0 1076(1)	0 2233(2)	2 97(5)
C(3)	0 5549(3)	0.2387(2)	0 1298(2)	3.33(7)
C(4)	0 4407(3)	0.2755(2)	0 0370(2)	3 31(7)
C(5)	0 4690(3)	0.3508(2)	−0.0458(3)	4.38(9)
C(6)	0.6053(4)	0 3869(2)	−0.0386(3)	5.1(1)
C(7)	0 7184(3)	0 3510(3)	0 0499(3)	5.3(1)
C(8)	0 6927(3)	0.2782(2)	0.1339(3)	4.56(9)
C(Me1)	0.0444(3)	0 1518(3)	0.0896(4)	5 6(1)
C(Me2)	0 3000(4)	0.0390(3)	−0.1085(3)	5.9(1)

tin atom has been observed in [*N*-(2-mercaptophenyl)-salicylideneaminato-*N*,*O*,*S*]dimethyltin(IV) [14].

Even though the coordination scheme is basically the same in both complexes, a close look at the bond distances and bond angles (Tables 4 and 5) shows certain differences. In the phenyl derivative the Sn–O distance is shorter and the Sn–S bond slightly longer than in the methyl complex, possibly due to the $SnPh_2$ moiety being 'harder' [15] than $SnMe_2$ because of the greater electronegativity of the phenyl group [16]. Also, the angle N–Sn–O [15] is slightly wider in the phenyl complex.

The main changes in the free ligand structure [17] under coordination are those usually accompanying the formation of metallic thiosemicarbazonates, and can be described as follows: (i) a 180° rotation about N(2)–C(1) that switches the positions of N(1) and S (giving a Z configuration about the C(1)–N(2) bond) and thereby allows the sulfur atom to form a five-membered chelate ring with the metal and N(3); (ii) modifications in bond distances and bond angles in the thiocarbamide group, namely the lengthening of C(1)–S (thione–thiol evolution) and C(1)–N(1) (reduction in the resonance contribution of R–CH=N–NH–C(S^-)$=NH_2^+$), shortening of C(1)–N(2) (increase in bond order), widening of S–C(1)–N(2) and narrowing of the other two angles at C(1); (iii) narrowing of C(1)–N(2)–N(3) (probably because the bonding pair involved in the N(2)–H bond of the free ligand becomes a lone pair in the complexes). In addition, the C(4)–O

TABLE 3 Positional parameters for $[SnPh_2(L)]$ with e s d s in parentheses

Atom	x/a	y/b	z/c	B_{iso}
Sn	−0 0050(1)	0 2449(1)	0 2423(1)	3 20(1)
S	0 0020(1)	0 1543(2)	0 0927(1)	4.70(4)
O	0 0380(3)	0.2871(4)	0.3825(2)	4 5(1)
N(1)	0 1762(3)	0 0519(5)	0.0843(3)	5 5(2)
N(2)	0 2073(3)	0 1348(4)	0 2276(3)	3 6(1)
N(3)	0 1674(3)	0.1969(4)	0 2872(2)	3.0(1)
C(1)	0 1377(4)	0.1107(5)	0 1430(3)	3 5(1)
C(2)	0 2434(4)	0 2241(4)	0 3679(3)	3 4(1)
C(3)	0 2325(4)	0.2837(4)	0 4473(3)	3 3(1)
C(4)	0 1327(4)	0.3141(5)	0 451(3)	3 4(1)
C(5)	0 1314(4)	0 3716(5)	0 5330(3)	4 1(2)
C(6)	0 2279(5)	0 3967(5)	0 6076(3)	4 7(2)
C(7)	0 3271(5)	0.3685(6)	0.6038(3)	5.2(2)
C(8)	0 3289(4)	0 3115(6)	0.5251(3)	4 8(2)
C(9)	−0 1149(4)	0 0987(5)	0 2499(4)	3 8(2)
C(10)	−0 2015(4)	0 0603(6)	0 1686(4)	5 0(2)
C(11)	−0 2767(5)	−0 0322(7)	0 1722(5)	6 5(2)
C(12)	−0 2681(5)	−0 0824(7)	0 2553(6)	6 6(3)
C(13)	−0 1842(6)	−0 0484(6)	0 3363(5)	5 9(2)
C(14)	−0 1059(4)	0.0443(5)	0 3341(4)	4 8(2)
C(15)	−0 0411(3)	0.4457(5)	0.1988(3)	3 4(1)
C(16)	−0 0572(4)	0.4857(5)	0 1085(3)	4 2(2)
C(17)	−0 0807(5)	0 6185(6)	0 0823(4)	5 6(2)
C(18)	−0 0868(5)	0 7103(6)	0.1456(6)	6.5(2)
C(19)	−0 0702(5)	0 6706(6)	0.2348(5)	6 0(2)
C(20)	−0 0482(4)	0.5393(5)	0 2615(4)	4 4(2)

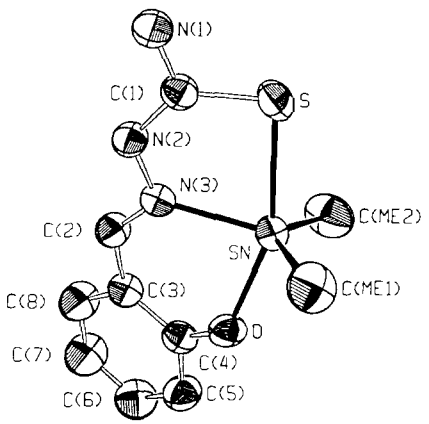

Fig 1 The structure of $[SnMe_2(L)]$, with the atom-numbering scheme

bond becomes shorter upon deprotonation and complex formation, suggesting a participation of this bond in the π charge delocalization induced by the metalation

There are also differences in ligand structure between $[SnMe_2(L)]$ and $[SnPh_2(L)]$. For example, changes (i) are larger in the phenyl derivative (except for the narrowing of N(1)–C(1)–N(2), for which the difference is of the order of the e.s.d.s). More conspicuously, the ligand is rather planar in $[SnPh_2(L)]$ (for the least-squares plane through N(1), S, C(1), N(2), N(3), C(2),

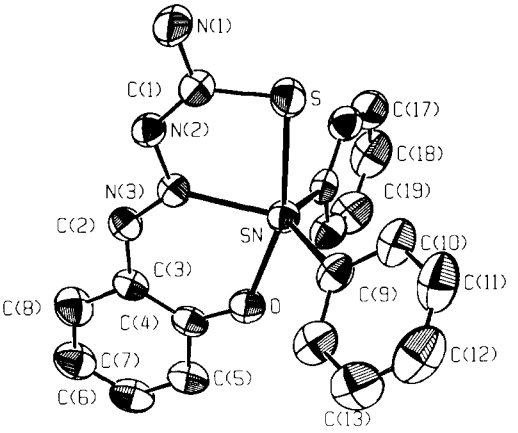

Fig 2. The structure of $[SnPh_2(L)]$, with the atom-numbering scheme

TABLE 4 Bond distances (Å) and angles (°) for $[SnMe_2(L)]$

Sn–S	2.5425(8)	C(1)–N(2)	1 312(3)
Sn–N(3)	2 199(2)	C(2)–C(3)	1 434(3)
Sn–O	2 111(2)	C(3)–C(4)	1 413(3)
Sn–C(Me1)	2.103(3)	C(4)–C(5)	1 399(4)
Sn–C(Me2)	2.125(3)	C(6)–C(7)	1 377(5)
S–C(1)	1 724(3)	C(3)–C(8)	1 405(4)
C(1)–N(1)	1.337(3)	C(5)–C(6)	1 371(5)
C(2)–N(3)	1 300(3)	C(7)–C(8)	1.375(5)
N(2)–N(3)	1 384(3)	O–C(4)	1.329(3)
S–Sn–O	158 10(5)	N(3)–C(2)–C(3)	126 9(2)
S–Sn–N(3)	76 87(5)	C(1)–N(2)–N(3)	116.4(2)
S–Sn–C(Me1)	97 93(9)	Sn–N(3)–C(2)	124 6(2)
S–Sn–C(Me2)	97 5(1)	Sn–N(3)–N(2)	121 0(1)
O–Sn–N(3)	81 66(7)	C(2)–N(3)–N(2)	114 2(2)
O–Sn–C(Me1)	88 7(1)	C(2)–C(3)–C(4)	123 8(2)
O–Sn–C(Me2)	94 8(1)	C(2)–C(3)–C(8)	117 5(2)
N(3)–Sn–C(Me1)	119 0(1)	C(4)–C(3)–C(8)	118 7(2)
N(3)–Sn–C(Me2)	113.3(1)	O–C(4)–C(3)	121 4(2)
C(Me1)–Sn–C(Me2)	127.5(1)	O–C(4)–C(5)	119 9(2)
Sn–S–C(1)	95 50(9)	C(3)–C(4)–C(5)	118.7(2)
Sn–O–C(4)	126 7(1)	C(4)–C(5)–C(6)	120 6(3)
S–C(1)–N(1)	116.6(2)	C(5)–C(6)–C(7)	121 6(3)
S–C(1)–N(2)	126 6(2)	C(6)–C(7)–C(8)	118.8(3)
N(1)–C(1)–N(2)	116 8(2)	C(3)–C(8)–C(7)	121 6(3)

C(3), C(4) and O, $\chi^2 = 8178.2$) and forms a dihedral angle of 86.5° with the equatorial plane (N(3), C(9), C(15), Sn, $\chi^2 = 86.5$). This planarity is to a great extent lost in the methyl complex (for the least-squares plane through N(1), S, C(1), N(2), N(3), C(2), C(3), C(4) and O, $\chi^2 = 230893.4$) in which the equatorial plane (N(3), C(Me1), C(Me2), Sn) is also less perfect ($\chi^2 = 593.2$).

The hydrogen bond network of H_2L [17] is obviously altered upon complexation. Intramolecular O–H...N(3) and N(1)–H...N(3) bonds and the intermolecular N(2)–H ..S bond disappear due to the deprotonation of O and N(2) and the rotation of the thioamide group about the N(2)–C(1) bond. However an intermolecular

TABLE 5. Bond distances (Å) and angles (°) for $[SnPh_2(L)]$

Sn–S	2 546(1)	N(1)–C(1)	1 358(7)
Sn–O	2.072(3)	N(2)–N(3)	1 396(6)
Sn–N(3)	2 196(4)	N(2)–C(1)	1 300(6)
Sn–C(9)	2 127(5)	N(3)–C(2)	1 295(6)
Sn–C(15)	2 128(5)	C(9)–C(14)	1 385(8)
S–C(1)	1.733(5)	C(10)–C(11)	1 395(9)
O–C(4)	1.327(6)	C(11)–C(12)	1.35(1)
C(2)–C(3)	1.438(6)	C(12)–C(13)	1 36(1)
C(3)–C(4)	1.406(8)	C(13)–C(14)	1 42(1)
C(3)–C(8)	1.406(7)	C(15)–C(16)	1 398(7)
C(4)–C(5)	1.407(7)	C(15)–C(20)	1 391(7)
C(5)–C(6)	1 378(8)	C(16)–C(17)	1 398(8)
C(6)–C(7)	1.39(1)	C(17)–C(18)	1 38(1)
C(7)–C(8)	1 366(8)	C(18)–C(19)	1 38(1)
C(9)–C(10)	1.391(8)	C(19)–C(20)	1 383(8)
S–Sn–O	161.1(1)	C(2)–C(3)–C(4)	124 1(4)
S–Sn–N(2)	55 91(8)	C(2)–C(3)–C(8)	116 7(4)
S–Sn–N(3)	77 9(1)	C(4)–C(3)–C(8)	119 1(4)
S–Sn–C(9)	94 9(1)	O–C(4)–C(3)	123 0(4)
S–Sn–C(15)	97 8(1)	O–C(4)–C(5)	117 5(4)
O–Sn–N(2)	105 7(1)	C(3)–C(4)–C(5)	119.4(4)
O–Sn–N(3)	84 0(1)	C(4)–C(5)–C(6)	119 4(5)
O–Sn–C(9)	89 4(2)	C(5)–C(6)–C(7)	121 6(5)
O–Sn–C(15)	94 2(2)	C(6)–C(7)–C(8)	119 3(5)
N(2)–Sn–N(3)	22 0(1)	C(3)–C(8)–C(7)	121 2(5)
N(2)–Sn–C(9)	115 6(2)	C(10)–C(9)–C(14)	118.6(5)
N(2)–Sn–C(15)	114 1(1)	C(9)–C(10)–C(11)	120.4(6)
N(3)–Sn–C(9)	120.1(2)	C(10)–C(11)–C(12)	120.3(6)
N(3)–Sn–C(15)	112.9(2)	C(11)–C(12)–C(13)	121.1(7)
C(9)–Sn–C(15)	127.0(2)	C(12)–C(13)–C(14)	119.5(6)
Sn–S–C(1)	95.5(2)	C(9)–C(14)–C(13)	120 0(5)
Sn–O–C(4)	132.0(3)	C(16)–C(15)–C(20)	119 2(5)
Sn–N(3)–N(2)	121 8(3)	C(15)–C(16)–C(17)	119.8(5)
Sn–N(3)–C(2)	125 9(3)	C(16)–C(17)–C(18)	120.2(6)
N(3)–N(2)–C(1)	116 6(4)	C(17)–C(18)–C(19)	119 8(7)
N(2)–N(3)–C(2)	112.2(4)	C(18)–C(19)–C(20)	120 7(6)
S–C(1)–N(1)	115 1(4)	C(15)–C(20)–C(19)	120 2(5)
S–C(1)–N(2)	127 8(4)	N(1)–C(1)–N(2)	116 9(4)
N(3)–C(2)–C(3)	127 8(4)		

N(1)–H...O bond remains in $[SnMe_2(L)]$ (O...N(1)' = 2.882(3), O...H(N(1))' = 2.021(2), N(1)'–H = 0.835(2) Å, O...H(N(1))'–N(1)' = 159.6(2)°, where N(1)' is generated by the symmetry operation ($\frac{1}{2}-x$, $\frac{1}{2}+y$, $\frac{1}{2}-z$). In $[SnPh_2(L)]$ this bond is replaced by a weak interaction between the S atom and the $-N(1)H_2$ group (S...N(1)' = 3.522, S...H(N(1))' = 2.612(2), N(1)'–H = 0.968(4) Å, N(1)'–H(N(1)')...S = 156.6(3)°).

Mass spectra

Table 6 lists the most relevant ions detected in the EI mass spectra. Both spectra show the molecular ions, suggesting appreciable stability under electron impact in the thermal conditions used. According to the peak intensities, $[SnPh_2(L)]$ is more stable than $[SnMe_2(L)]$. In general, the fragmentation pathways of the two complexes are similar and consistent with the mechanism proposed for the ionization of $[SnBu_2(L)]$ [3a], although

TABLE 6. Main peaks in the IE mass spectra of $[SnMe_2(L)]$ and $[SnPh_2(L)]$

m/z	Intensity (rel.)	Assignment
$[SnMe_2(L)]$		
343	28	$[M]$
328	100	$[M-Me]$
313	73	$[M-2Me]$
254	15	$[C_7H_6N_2OSn]$
238	18	$[C_7H_5NOSn]$
135	19	$[SnCH_3]$
120	3	[Sn]
119	14	$[C_7H_5NO]$
118	27	$[C_7H_4NO]$
$[SnPh_2(L)]$		
467	48	$[M]$
390	100	$[M-Ph]$
313	14	$[M-2Ph]$
280	10	$[M-2Ph-S]$
238	20	$[C_7H_5NOSn]$
197	29	[SnPh]
120	15	[Sn]
119	10	$[C_7H_5NO]$
118	11	$[C_7H_4NO]$

TABLE 7. Main IR bands of the ligand and complexes (cm^{-1})

H_2L	$[SnMe_2(L)]$	$[SnPh_2(L)]$	Assignment
3440s	3320s, b	3440s	ν(NH), ν(OH)
3320s	3145s, b	3315s	
3160s, b			
3120m			
1610s	1650s	1600s	$\delta(NH_2)$
1600s	1600s	1590s	ν(C=N)
1280m	1290m	1300m	ν(C–O)
1060m	1040m	1040m	ν(C=S)
830m	820m	820m	
	560m	280m[a]	ν_{as}(Sn–C)

[a] + ligand band.

in the spectra of the methyl and phenyl derivatives the base peak is the fragment [M – R] not the $[C_7H_5NOSn]$ ion. The cleavage of the $NC(S)NH_2$ fragment (and the Sn–S bond) while the Sn–O and Sn–N bonds remain is in keeping with the bond strength sequence indicated by the X-ray study (*vide supra*) and with the fragmentation sequence for the butyl analogue suggested by Tandon *et al.* [3a]

IR spectra

Table 7 shows the assignment of the main IR bands of the ligand and the complexes. In the region 3500–3100 cm^{-1}, H_2L shows four bands attributed [18–21] to ν(N–H) and ν(O–H) of the hydrogen bonded NH_2, N–H and O–H groups [17]. As a result of the double deprotonation of the ligand, the spectrum of the complex $[SnPh_2(L)]$ lacks the bands located at smaller wave-

numbers but retains those attributed to the $-NH_2$ group practically unchanged at 3440 and 3315 cm^{-1}, in keeping with the amine group of the phenyl complex being involved in weak hydrogen bond interactions but not in coordination to the metal. The spectrum of $[SnMe_2(L)]$ in this region is different, showing two broad bands shifted to smaller wavenumbers than in the free ligand spectrum. These shifts and that of $\delta(NH_2)$ to higher wavenumbers, are probably due to the hydrogen bond in which the NH_2 group is involved being stronger than in $[SnPh_2(L)]$ (see the X-ray results).

The coordination of N(3) does not significantly change the position of ν(C=N); O-coordination shifts ν(C–O) to slightly higher wavenumbers, while S-coordination shifts the bands contributed to by ν(C=S) to lower wavenumbers. This behaviour is typical for this ligand when it is N,S,O-coordinated [19–21].

Although the complexity of the ligand spectrum in the 600–200 cm^{-1} range makes it difficult to interpret changes in this region and masks some bands due to the organometallic moieties (e.g. ν_{sym}(Sn–C)), it seems likely that new bands in the range 400–300 cm^{-1} (at 385 and 350 cm^{-1} for $[SnPh_2(L)]$ and at 380 and 340, 330 cm^{-1} for $[SnMe_2(L)]$), though not pure, are contributed to by ν(Sn–N) and ν(Sn–S).

Mossbauer spectra

In keeping with the X-ray results, the isomer shift values and quadrupole splitting values of the complexes (Table 8) are consistent with diorganotin(IV) compounds with pentacoordinate geometries, and the narrow linewidths are indicative of the presence of a single tin site. The quadrupole splitting values deserve some comment because they are much lower than those calculated by the simple symmetrization method [22] (3.28 and 2.70 mm/s for the methyl and phenyl derivatives, respectively). This fact seems to imply a large effect of the thiosemicarbazonate anion on the electron distribution among the tin p-orbitals. Moreover, it was not possible to fit the spectrum of $[SnMe_2(L)]$ to a simple quadrupole doublet; only a continuous distribution of ΔE_Q values gave acceptable results (the value listed in Table 8 is the most probable). This behaviour may be related to the non-planarity of the thiosemicarbazone moiety in the monocrystal studied by X-ray diffraction (it is planar in the diphenyl derivative); it is possible that a polycrystalline sample contains molecules with a variety of different conformations, each of which gives rise to a slightly different Mössbauer spectrum.

TABLE 8. Mossbauer parameters at 80 0 K (mm/s)

Compounds	δ	ΔE_Q	Γ
$[SnMe_2(L)]$	1.27	2.43	0 80
$[SnPh_2(L)]$	1.30	2 30	0.99

NMR spectra

Both complexes are soluble in chloroform, even though the solubility of the ligand in this solvent is very slight. The changes in the ^1H NMR spectrum of H_2L under complexation are as follows: (i) deprotonation of the ligand supresses the –OH and –N(2)–H singlets appearing at 9.87 and 11.38 ppm in the spectrum of H_2L in DMSO-d_6; (ii) the –C(2)–H proton is deshielded, appearing at 8.51 and 8.54 ppm in $[SnMe_2(L)]$ and $[SnPh_2(L)]$, respectively (in $CDCl_3$), as against 8.36 ppm in H_2L (in DMSO-d_6); (iii) the two $-NH_2$ protons, which appear at 8.12 and 7.89 ppm in the spectrum of H_2L in DMSO-d_6, become magnetically equivalent in the complexes, probably due to the reduction in C(1)–N(1) bond order indicated by the X-ray study (*vide supra*) and to the rupture of the intramolecular hydrogen bond N(1)–H.. N(3) [17] when the conformation of the ligand is modified upon complexation (*vide supra*).

Table 9 shows the most relevant ^{13}C and ^{119}Sn NMR data. Due to scant solubility of H_2L in $CDCl_3$, its spectrum was recorded in DMSO-d_6. To find out the influence of the solvent, spectra were recorded for $[SnMe_2(L)]$ in both $CDCl_3$ and DMSO-d_6. The change of solvent shifts the carbon signals only slightly (by $\leqslant 1.1$ ppm), except for the C(2) signal, which in DMSO-d_6 solution lies 3.4 ppm upfield of its position in $CDCl_3$ (see Table 9).

C(1) is more shielded in the complexes than in the free ligand, suggesting that the shielding effect [23] due to the thione–thiol evolution of the C(1)–S group and to the reinforcement of C(1)–N(2) bond order outweigh the deshielding inductive effect of the S–Sn bond. Note that C(1) is deshielded upon formation of $[Cd(PyTSC)_2]$ (PyTSC = 2-formylpyridine thiosemicarbazonate) [8], this difference with respect to the tin complexes possibly being ascribable to the sulfur–metal bond being stronger than in the latter.

C(2), and to a lesser extent C(4), are strongly deshielded by complexation. The C(2) signals show weak satellite peaks (at 20.8 and 20.6 Hz for $[SnMe_2(L)]$ and $[SnPh_2(L)]$, respectively) that may derive from carbon–tin coupling through the N(3) atom as proposed in Table 9.

Substitution of the value of $^1J(^{13}C–^{119}Sn)$ (Table 9) in the Lockhart–Manders equation [24] yields a C–Sn–C angle of *c.* 132° for the dimethyltin(IV) complex, in reasonable agreement with the angle observed in the solid state (Table 4). $^2J(^1H–^{119}Sn)$ for this compound (70.0 Hz) is in the usual range for pentacoordinated compounds.

TABLE 9 ^{13}C and ^{119}Sn NMR spectral data (δ, ppm, J, Hz) of the ligand and complexes[a]

Complex	Solvent	δ[C(1)]	δ[C(2)]	δ[C(3)]	δ[C(4)]	δ[C(5)]	δ[C(6)]	δ[C(7)]	δ[C(8)]	δ[MR$_n$]	^nJ(R–$^{117/119}$Sn)	^2J(C(2)–Sn)	δ[Sn]
H_2L	DMSO-d_6	177 87	139.98	120 35	156 49	116 12	131.14	119 34	126 91				
[$SnMe_2$(L)]	$CDCl_3$	167 98	161 29	116 91	166 26	117 28	134 84	121 62	132 79	5 92	627 7/600 4	20 8	– 104 7
	DMSO-d_6	168 07	157 89	116 54	165 77	117 93	133 99	121 12	133 88	7 77			
[$SnPh_2$(L)]	$CDCl_3$	166 92	161.23	116 93	166 31	117 49	135 07	121 82	133 91	142 6 i		20 6	– 235 4
										135 9 o	56 3		
										128 7 m	81 2/84 3		
										130 1 p	17 0		

[a]Numbering scheme see Figs 1 and 2

All these data suggest that the basic characteristics of the solid-state structures of the complexes remain in $CDCl_3$ solution.

^{119}Sn chemical shifts have been found to be influenced by several factors [25], and at present their interpretation is limited to an essentially qualitative level [26]. ^{119}Sn resonances located between −90 and −330 ppm have been empirically related to five-coordination of the tin atom [27] in methyltin derivatives. The value for [$SnMe_2$(L)] (Table 9) is inside this range but at its lower limit. Perhaps the presence of S and N atoms in the coordination sphere of the tin shifts the signal towards more deshielded values; indeed S- or N-bonded dimethyltin(IV) compounds often have positive ^{119}Sn chemical shifts [25]. In [$SnPh_2$(L)] the ^{119}Sn signal lies, as usual [28], at lower frequencies than in [$SnMe_2$(L)], in spite of the greater electron withdrawing capability of the phenyl group.

Acknowledgement

We thank the DGICYT (Spain) for financial support under Project PS90-0195.

References

1 D.X West, S.B. Padhye and P.B. Sonawane, *Struct Bonding (Berlin), 76* (1991) 1
2 A H. Penninks, P.M. Punt, M. Bol-Schoenmakers, H.J.M van Rooijen and W. Seinen, *Silicon, Germanium, Tin, Lead Comp, 9* (1986) 367.
3 (a) A.K. Saxena, J.K. Koacher and J.P Tandon, *Inorg Nucl Chem Lett, 17* (1981) 229; (b) A. Saxena and J.P. Tandon, *Inorg Chim Acta, 84* (1984) 195; (c) *Polyhedron, 3* (1984) 681; (d) A. Varshney and J.P. Tandon, *Ind J Chem, 24A* (1985) 70, (e) *Polyhedron, 5* (1986) 739.
4 (a) M. Nath, N. Sharma and C L Sharma, *Synth React. Inorg Met -Org Chem, 19* (1989) 339; (b) *20* (1990) 623
5 (a) F.E. Anderson, C.J. Duca and J V Scudi, *J Am Chem Soc, 73* (1951) 4967; (b) R S. Tobias, I Ogrins and B.A. Nevett, *Inorg Chem, 1* (1962) 638
6 D. Stuart and N Walker, *Acta Crystallogr, Sect. A, 39* (1983) 158
7 M.V. Castaño, M.M. Plasencia, A Macías, J.S Casas, J. Sordo and E E. Castellano, *J Chem Soc, Dalton Trans,* (1989) 1409
8 R.F Stewart, E R Davidson and W.T Simpson, *J Chem Phys, 42* (1965) 3175.
9 J S Casas, M.V Castaño, M.S. García-Tasende, I Martínez-Santamarta, A. Sánchez, J Sordo, E E Castellano and J Zukerman-Schpector, *J Chem Res S,* (1992) 324, *J Chem Res M,* (1992) 2626.
10 R.T. Sanderson, *Inorganic Chemistry,* Reinhold, New York, 1967, p 74
11 S W Ng, V.G.K Das, B W. Skelton and A.H. White, *J Organomet Chem, 377* (1989) 211.
12 A Bondi, *J Phys Chem, 68* (1964) 441
13 M V Castaño, A. Macias, A Castiñeiras, A. Sánchez-González, E. García-Martínez, J S Casas, J Sordo, W. Hiller and E E. Castellano, *J Chem Soc, Dalton Trans.,* (1990) 1001, and refs therein
14 G Y. Yeap, H.K Fun, S B. Teo and S G. Teoh, *Acta Crystallogr, Sect C, 48* (1992) 1109.
15 R.G. Pearson, *Hard and Soft Acids and Bases,* Dowden, Hutchinson & Ross, Strondsburg, 1973
16 J E Huheey, *Inorganic Chemistry,* Harper & Row, Cambridge, 3rd edn., 1983, p 156
17 D. Chattopadhyay, S.K. Mazumdar, T. Banerjee, S Ghosh and T.C.W Mak, *Acta Crystallogr, Sect C, 44* (1988) 1025.
18 D.M. Wiles and T. Suprunchuk, *Can J Chem, 47* (1969) 1087.
19 V M Leovac, L. Bjelica and L. Jovanovic, *Polyhedron, 4* (1985) 233.
20 S.P Mital, R.V Singh and J.P. Tandon, *Synth React Inorg Met -Org Chem, 11* (1981) 547
21 M N. Mokerjee, R.V. Singh and J.P Tandon, *Synth React Inorg. Met -Org Chem, 15* (1985) 13
22 R.V. Parish, in G J. Long (ed.), *Mossbauer Spectroscopy Applied to Inorganic Chemistry,* Plenum, New York, 1984, Ch. XI, p. 544
23 A.M. Brodie, H D. Holden, J. Lewis and M.J Taylor, *J Chem. Soc, Dalton Trans,* (1986) 633.
24 T.P Lockhart and W.F Manders, *Inorg Chem, 25* (1986) 892.
25 R.K Harris, J.D Kennedy and W. McFarlane, in R.K. Harris and B E Mann (eds.), *NMR and the Periodic Table,* Academic Press, London, 1978, pp 342
26 R Hani and R A. Geanangel, *Coord Chem Rev, 44* (1982) 229
27 J Otera, *J. Organomet Chem, 221* (1981) 57.
28 P J. Smith and A P. Tupciauskas, *Annu. Rep NMR Spectrosc, 8* (1978) 291